Available online at www.sciencedirect.com

ScienceDirect

journal homepage: www.elsevier.com/locate/issn/15375110

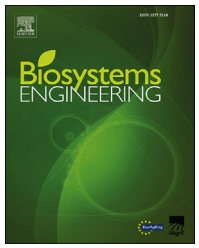

Special Issue: Robotic Agriculture

Research Paper

Selective spraying of grapevines for disease control using a modular agricultural robot

Roberto Oberti [a,*], *Massimo Marchi* [a,b], *Paolo Tirelli* [a,b], *Aldo Calcante* [a], *Marcello Iriti* [a], *Emanuele Tona* [a], *Marko Hočevar* [c], *Joerg Baur* [d], *Julian Pfaff* [d], *Christoph Schütz* [d], *Heinz Ulbrich* [d]

[a] *Dept. Agricultural and Environmental Science – DiSAA, Università degli Studi di Milano, via Celoria 2, 20133 Milano, Italy*

[b] *Applied Intelligent Systems–AIS Lab, Dipartimento di Informatica, Università degli Studi di Milano, via Celoria 26, 20133 Milano, Italy*

[c] *University of Ljubljana, Faculty of Mechanical Engineering, Aškereeva 6, SI 1000 Ljubljana, Slovenia*

[d] *Institute of Applied Mechanics, Technische Universität München, Boltzmannstr. 15, 85748 Garching, Germany*

ARTICLE INFO

Article history:
Published online 13 January 2016

Keywords:
Precision spraying
Agricultural robot
Crop protection
Automation
Disease sensing

Due to their recognised role in causing environmental pressures, the need to reduce production costs and public concerns over the healthfulness of fresh products and food, reducing pesticide use in agriculture is a major objective. In current farming practice, pesticides are typically applied uniformly across fields, despite many pests and diseases exhibiting uneven spatial distributions and evolving around discrete foci. This is the fundamental rationale for implementing the selective targeting of pesticide applications such that pesticides are deposited only where and when they are needed and at the correct dose. This approach is explored using the example of powdery mildew on grape vines controlled by means of a modular agricultural robot developed within the EU-project CROPS. The CROPS manipulator was configured to six degrees of freedom and equipped with a new precision-spraying end-effector with an integrated disease-sensing system based on R-G-NIR multispectral imaging. The robotic system was tested on four different replicates of grapevine canopy plots (5 m in length × 1.8 m in height) prepared in a greenhouse setup by aligning potted plants exhibiting different levels of disease. The results indicate that the robot was able to automatically detect and spray from 85% to 100% of the diseased area within the canopy and to reduce the pesticide use from 65% to 85% when compared to a conventional homogeneous spraying of the canopy. This work, to the best of our knowledge, is the first using a totally automatic selective system for spraying of diseases in specialty crops.

* *Corresponding author.*
E-mail address: roberto.oberti@unimi.it (R. Oberti).

http://dx.doi.org/10.1016/j.biosystemseng.2015.12.004
1537-5110/

Nomenclature

CAN	controller area network
CCU	central control unit
CROPS	clever robots for crops project
DoF	degree of freedom
EU	European Union
PWM	pulse width modulation
R-G-NIR	red, green, near-infrared (spectral channels)
ROI	region of interest (of an image)
ROS	robot operating system
TCP	tool-centre-point (frame of reference)
VIS-NIR-MIR	visible, near-Infrared, mid-infrared (spectral bands)

Symbols

x	axis defined by the robot traveling direction (parallel to the canopy wall)
y	axis defined by the front direction from the robot to the canopy
z	vertical axis
α	latitude angle defined by rotations around the x−axis
γ	longitude angle defined by rotations around the z−axis

1. Introduction

In recent decades, the reduction of pesticide use in agriculture has been a major objective of EU policy; it was one of the strategic themes of the 6th Environment Action Programme and the topic of a framework directive on sustainable pesticide use (2009/128/EC). Indeed, pesticides are recognised to play a major role in environmental pressure (Sabatier et al., 2014; Stehle & Schulz, 2015), agricultural production costs and public concerns about the healthfulness and wholesomeness of fresh products (Abdollahi, Ranjbar, Shadnia, Nikfar, & Rezaie, 2004; Burns, McIntosh, Mink, Jurek, & Li, 2013; Rauh et al., 2012).

The objective of reducing pesticide use has been tackled through different and complementary approaches, including selection of resistant varieties, crop management techniques, crop scouting practices, application of biocides and beneficial organisms, and regular maintenance and optimal setting of spraying equipment.

In current farming practice, pesticides are typically applied uniformly to fields. However, several pests and diseases exhibit an uneven spatial distribution, with typical patch structures evolving around discrete foci (localised areas exhibiting symptoms), especially during early stages of development (Everhart, Askew, Seymour, & Scherm, 2013; Spósito, Amorim, Bassanezi, Filho, & Hau, 2008; Waggoner & Aylor, 2000).

This is the fundamental rationale for implementing selective spraying capability by means of highly automated equipment or robots. Such systems would enable the selective targeting of pesticide application only where and when it is needed, with the aim of controlling the initial foci and preventing the infection establishment and its epidemic spread to the whole field (West et al., 2003).

This approach has been explored within the EU-funded project CROPS (www.crops-robots.eu), which is aimed at developing, optimising and demonstrating a highly modular and reconfigurable robotic system for accomplishing multiple agricultural operations, including selective spraying, ripeness monitoring and selective harvesting. This system is also able to work on different specialty crops, such as grapes, sweet peppers and apples (Baur, Pfaff, Ulbrich, & Villgrattner, 2012; Bontsema et al., 2014; Schütz, Pfaff, Baur, Buschmann, & Ulbrich, 2014).

The approach adopted in CROPS was clearly different from previous research on robotic agriculture, which typically relies on adaptation of non-modular, heavy standard industrial manipulators (e.g. Baeten, Donné, Boedrij, Beckers, & Claesen, 2008; Katupitiya, Eaton, Cole, Meyer, & Rodnay, 2005) or focuses on specific types of produce and operational tasks (e.g. Bac, van Henten, Hemming, & Edan, 2014; Guo, Zhao, Ji, & Xia, 2010; Hayashi et al., 2010; Van Henten et al., 2003). A few examples of multipurpose agricultural robotic systems have nevertheless been developed and tested especially for greenhouse operations (Belforte, Deboli, Gay, Piccarolo, & Ricauda Aimonino, 2006; Hayashi, Yoshida, Yamamoto, Iwasaki, & Urushiyama Miyagi, 2008; Mandow et al., 1996).

Over the past two decades, the idea of automated selective spraying (or spot spraying) has been introduced and investigated for herbicide applications (Felton & McCloy, 1992; Paice, Miller, & Day, 1996; Slaughter, Giles, & Tauzer, 1999), and this research has led to the development of some examples of currently available commercial equipment.

Although the concept was extended to crop-disease management (Larbi et al. 2013; Li, Xia, & Lee, 2009; Moshou et al., 2011; West et al., 2003), automated, selective spraying for diseases has not yet been developed. The reason is mainly that there have been only limited advances in automated detection systems for disease symptoms. Even if this is currently a blossoming field of research, a huge potential for improvement remains.

Sensor technologies for crop diseases have been extensively reviewed recently by Sankaran, Mishra, Ehsani, and Davis (2010), while a more focused discussion of the applications of proximal optical sensing for disease detection in arable crops can be found in West et al. (2003) and Mahlein, Oerke, Steiner, and Dehne (2012); a similar discussion for specialty crops can be found in Lee et al. (2010).

Among other case studies, grapevine is a perfect candidate crop to explore the concept of selective and targeted spraying of initial disease foci. Indeed, in current practice in viticulture, pesticide spraying is applied uniformly through the vineyard using a continuous protection approach throughout the growing season. For some of the most advanced wine-producing regions worldwide, this results in ten to fifteen or more applications per season, often conducted at high volume rates (typically 1000 l ha^{-1} or greater). A successful implementation of a timely detection system and the selective spraying of disease foci may have a dramatic impact on the amount of pesticide necessary to prevent an infection's establishment and its epidemic spread to the vineyard.

In this research we investigated the possibility of automatically detecting the symptoms of powdery mildew, a major fungal grapevine disease, and of selectively spraying the diseased canopy areas by means of the CROPS modular robot, equipped with a precision-spraying end-effector. The evaluations were based on deposition of spray on targets, with the implicit assumption that the treatment has contact action on the disease. The evaluation of the biological efficacy for different modes of action of the protection treatment is beyond the goal of this particular work.

The paper describes the components and the architecture of the robotic system, and details the methods and results of the experiments conducted in a demonstrating yet realistic crop scenario.

To the best of our knowledge, this is the first test conducted on totally automatic, selective spraying of diseases in specialty crops.

2. The robot system

The robot system used for the experiments was based on a CROPS manipulator configured to six degrees of freedom (DoFs); a precision-spraying end-effector and pesticide liquid-circuit; and a disease-sensing system. All the components were integrated thanks to an electronics and communication framework architecture.

2.1. *Manipulator*

The CROPS manipulator is a robotic arm with up to nine DoFs which is designed for different agricultural applications and operational environments. The manipulator has an overall mass of about 65 kg (depending on the chosen configuration) and is 1610 mm high, 480 mm wide and 670 mm long (minimum size in rest position).

In order to meet the requirements of a specific application, the arm has a highly modular design allowing its components to be rearranged in different configurations. For the precision spraying experiments on grapevine, the main requirements for defining the manipulator's working space were:

- the manipulator travelling direction (x-axis) was parallel to the canopy wall;
- the typical operating front distance (y-axis) from the canopy was 0.5 m;
- the typical height (z-axis) of the canopy to be sprayed was 0.9 m;
- the end-effector had to spray the target area from different directions to improve the spray coverage;
- the end-effector (precision sprayer) was rotationally symmetric around the y-axis, so only the rotations around the z−axis (longitude angle γ) and the x−axis (latitude angle α) were relevant for this application; and
- cycle time was not considered a major issue for this first set of experiments.

Figure 1 shows a schematic representation of the six-DoF configuration adopted in this research. Compared to the full configuration of the arm, workspace was reduced and rotation capability around the y-axis was not available, but the manipulator could carry a higher payload at the end-effector. The first DoF was obtained with a vertical prismatic joint, and the other five were revolute joints allowing movability in the x−z (joint 2) and y-z (joints 3–6) planes. Additionally, joint 1 and joints 3 to 5 were equipped with holding brakes to prevent the manipulator from collapsing under exceptional loads (Pfaff, Baur, Ulbrich, & Villgrattner, 2012 gives more details on the design of the CROPS manipulator).

In order to protect the electronics from spray liquid during the operation, a waterproof cover was made of

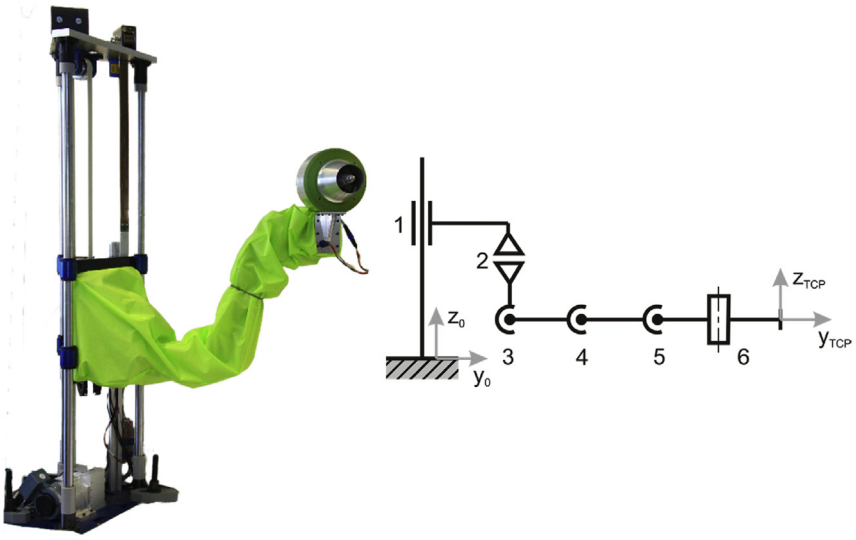

Fig. 1 – (a) CROPS manipulator with mounted precision-spraying end-effector and waterproof cover. (b) The manipulator's 6-DoF kinematic scheme; (y_o, z_o) is the body-fixed centre of the frame, and (y_{TCP}, z_{TCP}) is the TCP origin of the frame.

polyoxymethylene sheet perfectly fitted to the arm and enclosing the cabling used for power and data signals.

The installation of the protective cover resulted in coordinate limits of joint 2, being conservatively reduced to ±40° (instead of ±110°) in order to avoid mechanical restrictions and damage to the waterproof sheeting.

Moreover, since cycle time was not a major issue, the speed of all the joints was conservatively rated to limited values, as summarised in Table 1.

The manipulator's reachable workspace, i.e., the set of points that the robot can reach with at least one orientation, was computed by finding final poses of the tool-centre-point (TCP) frame with direct kinematics equations (Siciliano, Sciavicco, & Villani, 2009) while imposing the mechanical joint limits defined in Table 1. For the adopted configuration, the probability of self-collision of arm components was negligible and was not considered in the workspace analysis.

As shown by Fig. 2 (workspace computed for the specific case $a = 0$, i.e., no rotations about the x-axis), the manipulator could cover a range from 0 to 1.8 m in the z-direction thanks to the first prismatic joint. Moreover, depending on the desired orientation, the manipulator could reach positions from 0.4 to 1.1 m in the y-direction and from −0.5 m to +0.5 m in the x-direction.

The analysis indicated that the manipulator could cover the required workspace and was therefore suitable for the proposed application.

2.2. Precision spraying end-effector

The precision-spraying end-effector was a device designed to generate a pesticide liquid spray and a carrier airflow suitable to deliver spot-spraying patterns on target patches with a size limited to approximately 100–200 mm. The final implementation of the end-effector (Fig. 3) was in aluminium and plastic and had a total mass of 3.5 kg. The main components were: (1) an axial fan, (2) an airflow straightener, (3) an airflow cone, (4) a spray nozzle, (5) a pesticide control valve, and connections to the pesticide circuit and to the electronics.

The axial fan had dimensions of 120 × 120 × 38 mm and was powered by 48 V DC 2A supply. The fan rotational speed could be controlled in the range from 0 to 9500 rpm by a PWM signal. The airspeed was set according foliage density and thickness in order to obtain a proper flow penetration in the

Table 1 – Robotic manipulator joint specifications in the configuration used.

Joint	Speed		Joint coordinate limits		Force/Torque		Motor power
	Rated	Max	q_{min}	q_{max}	Rated	Max	Rated
1	1.2 m s^{-1}	2.5 m s^{-1}	−0.38 m	+0.46 m	303 N	596 N	880 W
2	254° s^{-1}	300° s^{-1}	−40°	+40°	14.5 N m	37 N m	70 W
3	225° s^{-1}	336° s^{-1}	−123°	−3°	103.5 N m	229 N m	250 W
4	195° s^{-1}	210° s^{-1}	−123°	+131°	57.5 N m	229 N m	250 W
5	143° s^{-1}	210° s^{-1}	−113°	+125°	30.0 N m	64 N m	70 W
6	397° s^{-1}	467° s^{-1}	−84°	+84°	9.5 N m	19 N m	70 W

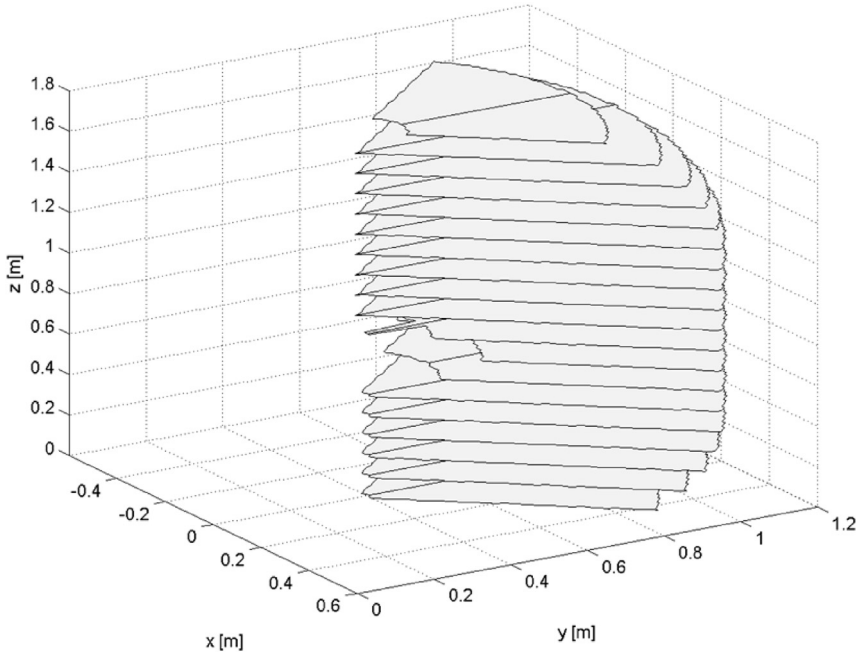

Fig. 2 – Manipulator workspace computed for latitude angle $\alpha = 0$.

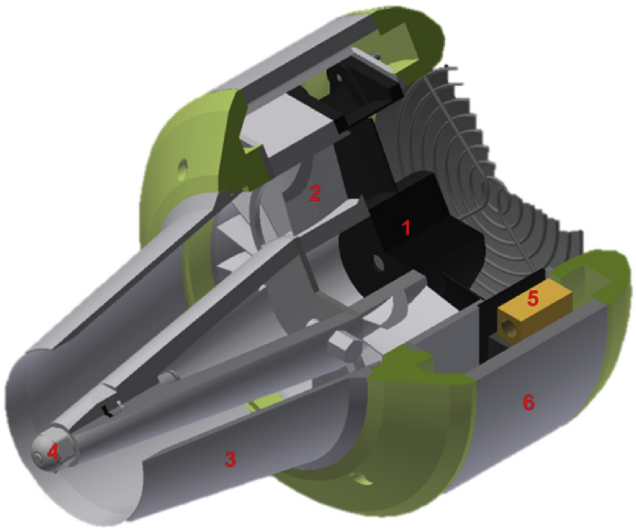

Fig. 3 – Cutaway diagram of precision-spraying end-effector: 1) axial fan, 2) flow straightener, 3) airflow nozzle, 4) pesticide nozzle, 5) pesticide valve, 6) chassis.

canopy. The axial fan allowed the generation of airflow with a maximum speed of about 20 m s^{-1}, when measured at a distance of 0.5 m from the spraying end-effector.

Immediately after exiting the fan, the airflow entered the flow straightener, which was designed to suppress swirl. This was a crucial component for maintaining the spatial confinement of the airflow and avoiding a broad spray plume of pesticide. The cone airflow tip was 126 mm long with an exit diameter of 80 mm. Inside the hollow air plume, a hollow-cone liquid-spraying nozzle was installed which delivered the pesticide mixture with a flow-rate of 18 ml min^{-1} when operating at nominal pressure of 350 kPa.

A direct-acting 3/2 solenoid valve controlled the opening and closing of the connection to the pesticide circuit, where liquid pressure was generated by an electric impeller pump installed in the manipulator base.

Laboratory measurements of the precision-spraying end-effector indicated that, at nominal pressure, the droplets volume median diameter at the exit from the end-effector was in the range of 200 μm as determined by water sensitive paper measurements, and the tangential component of the velocity vector in the airflow was negligible (below 1% of axial velocity component) as measured using rapid imaging techniques and a five-hole Pitot probe (Malneršič et al., 2012).

As an overall result of its design, the precision-spraying end-effector delivered a circular spray pattern of a quite constant diameter over a wide range of spraying distances, namely a diameter of 150 mm and of 200 mm was obtained at a spraying distance of 400 mm and of 1200 mm, respectively.

2.3. *Disease sensing system*

Among possible sensing techniques for disease-symptom detection, proximal optical sensing (conducted from a tractor or vehicle travelling the vineyard) has specific features especially relevant for field applications on grapevine and other specialty tree-crops (Oberti et al., 2014). In particular, proximal optical sensing can inspect the vertical structure of the canopy, allowing for potential on-the-go detection of early symptoms even at the centimetre scale and below.

The research dedicated to proximal optical detection of grapevine diseases is still limited to a few studies. Naidu, Perry, Pierce, and Mekuria (2009) investigated the potential of using reflectance changes in the VIS-NIR-MIR spectra of detached leaves to detect grapevine leafroll-associated virus (GLRaV-3) infection. Poutaraud et al. (2007) studied the detection of downy mildew (*Plasmopara viticola*) by means of in vivo fluorescence techniques, and Calcante, Mena, and Mazzetto (2012) evaluated two commercial optical devices in discriminating different infection levels on detached grapevine leaves.

The detection of powdery mildew (*Erysiphe necator*) was investigated by Bélanger, Roger, Cartolaro, Viau and Bellon-Maurel (2008) by means of fluorescence emission ratios and more recently by, Li, Ma, and Wang (2012) and Oberti et al. (2012, 2014) by means of imaging techniques. The latter studies demonstrated the potential of this technique's practical implementation in field conditions.

In this work, disease sensing was conducted by multispectral imaging of a grapevine canopy under diffuse illumination. Multispectral images of the canopy were acquired by a 3-CCD, R-G-NIR camera (MS4100, DuncanTech, Auburn, CA, USA). The camera captures 1912 × 1076-pixel, 8-bit images in three distinct spectral channels: green (540 nm), red (660 nm) and NIR (800 nm). The multispectral camera and a regular RGB camera (used for documentation but not for detection) were mounted on a sliding holder, allowing for positioning adjustments from 800 mm to 2500 m in height.

A holding frame, which is kept in a fixed position of the field of view three reflectance standard panels (Spectralon 20%, 50% and 99%, Labsphere, North Sutton, NH, USA) used to normalise the grey-level intensity of the pixels at different acquisitions. Stable and diffuse illumination of the imaged area was obtained by three diffusing panels containing a set of halogen lamps.

All the sensing equipment was installed in a frame beside the manipulator, resulting in a fixed longitudinal offset of 700 mm between the camera and the manipulator base. The same frame contained a sensing PC dedicated to data acquisition from the cameras, real-time image processing of multispectral images for disease detection, target position computation and transmission to the manipulator control computer.

2.4. *Electronics and communication architecture*

The main program control of the CROPS manipulator and the precision-spraying end-effector is implemented by a real-time control unit (xPC Target Matworks, Natick, MA, USA) hosted on the central control unit (CCU), a standard industrial PC with controller area network (CAN) interface boards (Fig. 4).

Aiming at a highly modular design, the open-source robotic middleware ROS robot operating system, Quigley et al. (2009) was chosen, allowing for the implementation of a modular user interface through several clients (e.g., a state monitor, a task planner or a viewer) to communicate with the robot system. The ROS interface application continuously

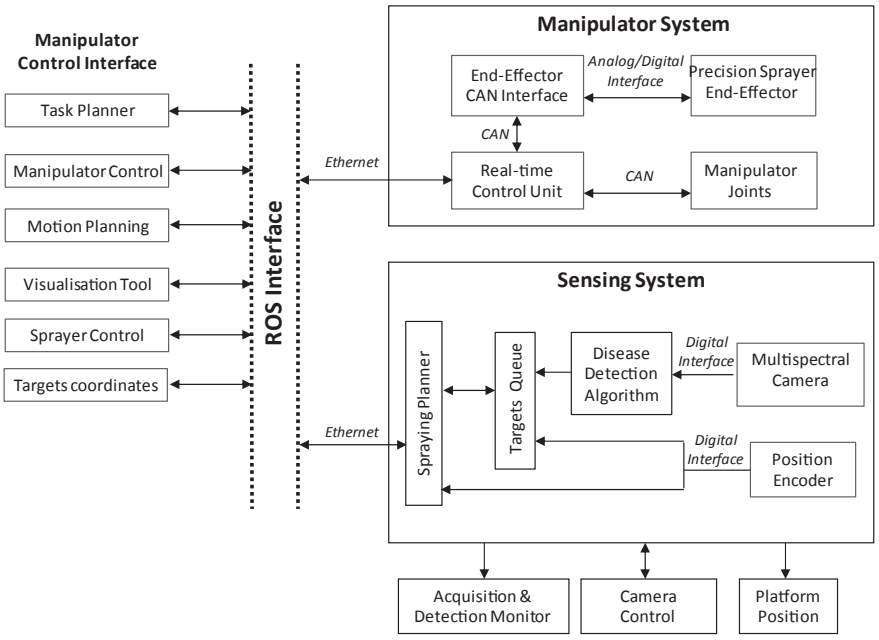

Fig. 4 – Hardware and software architecture of the robotic manipulator.

processes messages from and to the software framework containing information about the current status of the manipulator system (e.g., joint positions, end-effector positions, diagnostic messages and error messages).

The real-time control unit receives user commands via the ROS by custom-defined UDP messages. Operatively, this meant that the sensing PC, interfacing with the sensing cameras and running the disease-detection algorithms, computeds the target's position and sent the data (e.g., goal end-effector poses, airflow speed, and spraying commands) to the CCU. The data were processed in terms of inverse kinematics, trajectory planning, and self-collision checked to generate feasible joint position commands for the robot.

These position commands were sent via CAN (with $\Delta t = 5$ ms) to the manipulator's power-electronics, and they were then actuated by the joint motors. The sprayer commands (e.g., nozzle switch and fan speed) were sent via CAN to a small microcontroller board (AT90CAN32 Atmel, San Jose, CA, USA) mounted at the manipulator's link 4, providing several digital and analogue input/output channels for the control of the end-effector. For safety reasons, the main power supply could be automatically switched off by the real-time control unit.

3. Selective spraying experiments

3.1. *Plant material preparation and canopy setup*

In 2013, multiple sessions of greenhouse experiments were conducted on grapevine canopy with localised symptoms (i.e., disease foci) of powdery mildew (*Erysiphe necator*) to test the concept of automated, selective spraying to prevent crop diseases.

A relevant feature of powdery mildew is that the fungus colonises the adaxial (i.e. upper face) tissues of grapevine leaves by developing greyish branching filaments that possibly can expand to other green tissues, as young shoots and bunches. This infection mechanism makes powdery mildew an ideal case study for disease detection, even at an early stage, for a sensing system which frontally monitors the grapevine canopy.

To this aim, in spring 2012, 180 plants of *Vitis vinifera* (L. cv Cabernet Sauvignon) were propagated from wood and nursed in 300-mm-diameter pots in a greenhouse environment under controlled conditions at 25/20 °C day/night temperature, with 50–75% relative humidity and a 16 h photoperiod (40 μmol quanta m^{-2} s^{-1}). Grapevine plants were pruned in autumn so that they reached the full development stage during the experiment's schedule.

A subset of grown grapevine plants was inoculated by brushing *Erysiphe necator* conidia onto the adaxial (upper face) epidermis of healthy leaves in order to induce powdery mildew infection. The infected plants were nursed in a separated greenhouse room where favourable environmental conditions for disease development were maintained.

For the purpose of experimenting with the selective spraying system, the plant material was arranged in a greenhouse setup in order to simulate vineyard canopy conditions by aligning healthy grapevine plants in pots on nursery tables (Fig. 5). Within the prepared canopy wall, diseased plants with different levels of symptoms were positioned with the aim of simulating the presence of localised disease foci within healthy vegetation, representing the targets of selective spot spraying to be performed by the robot.

Different replicates of grapevine canopy plot (5 m in length × 1.8 m in height) were obtained by preparing different

Fig. 5 – The robotic setup (manipulator, sensing system and illuminators, control PCs) integrated on a wheeled platform during experiments of selective spraying on grapevine diseases in greenhouse.

plant arrangements, substituting healthy and diseased plants with other spare samples.

Robotic spraying tests were conducted at four different dates on four different canopy preparations. Prior to each test, a plant pathologist scouted the prepared canopy plot with an accurate visual inspection of the plants. Position, size and intensity of disease foci symptoms were recorded and used as ground-truth for subsequent assessment of the results obtained with each robotic spraying treatment.

3.2. *Robotic system setup and test procedure*

For the selective-spraying test session, all the different components of the robotic system were integrated on a wheeled trailer platform. An absolute encoder was mounted on one of the wheels, giving the position of the platform with a millimetre resolution along the travelling x-direction.

The manipulator body-fixed frame and the multispectral camera frame of reference were registered so that the position of a point at a known frontal distance y from the camera and having coordinates (x_i, z_i) in an acquired image could be univocally translated in a vector of coordinates (x_o, y_o, z_o) in the manipulator's frame of reference.

During all the tests, the platform holding the robotic system was positioned frontally to the canopy and, while travelling, the distance yov between the manipulator body-fixed frame and the midline of the vegetation was kept constant at 1.4 m. The camera was positioned at a fixed height of 1.45 m. The area covered by an image was about 0.5 m by 1.0 m, resulting in a spatial resolution of the multispectral image of about 0.5 mm pixel^{-1}.

To provide background regularisation and avoid multiple viewing across glass walls in the greenhouse, a black, low-reflective shield was positioned on the back of the prepared canopy.

The platform was moved in the x-direction at steps of 0.2 m, parallel to the canopy wall (i.e., at a constant y). At each position, a multispectral image of the canopy was acquired and processed in real-time (see below, disease detection algorithm).

Due to the ratio between the width of the sensed area (0.5 m) and the measurements step (0.2 m), each point of the canopy could be then imaged two or three times (depending on the considered canopy portion) from different positions. This enabled the robot to inspect a canopy area using multiple view directions to overcome possible partial occlusions of infection spots by healthy leaves being in front.

At each measurements step, the disease detection results in terms of presence and coordinates of symptoms, if any, were written in a spraying targets queue file.

Concurrently, at each step, if any previously identified targets in the queue file had a position in the canopy reachable by the manipulator at current platform standing, they were aggregated into single spraying spots (i.e., within circular regions of 150 mm in diameter). The centre-coordinates of each resulting spraying spot were then passed from the sensing PC to the manipulator's CCU through ROS messages. When the CCU answered back with a ROS message, the corresponding targets were assumed to have been sprayed by the robot and consequently deleted from the queue list.

In order to maximise the homogeneity of spray deposits and to enhance the reach and the covering of targets in deeper layers of leaves, each single spray spot (i.e., each identified 150-mm diameter circular region of the canopy) was sprayed from three different directions. For each spot to be sprayed, the manipulator was commanded to bring the end-effector in three poses; in each pose, the nozzle was operated to deliver one-third of the nominal volume of the spray dose (i.e., it is actuated for 0.5 s out of a total 1.5 s of spraying time). With this spraying sequence, each identified target spot receives, from three different directions, a spray amount corresponding to an application rate of about 35 ml m^{-2} of leaf area. Considering that grapevine canopies are generally managed to obtain a LAI (leaf area index) of 1.5–3 (depending on the growing region), the spraying rate used in our experiments was representative of application rates in the range of 500–1000 l ha^{-1} which are typical values for protection treatments in grapevine.

The sequence of the three poses of the end effector for each spray spot is: 1) distance of end-effector TCP from target spot's centre d = 0.6 m, latitude angle $\alpha = 30°$, longitude angle $\gamma = 0°$; 2) distance from spot's centre d = 0.6 m, latitude angle $\alpha = -30°$, longitude angle $\gamma = +30°$; 3) distance from spot's centre d = 0.6 m, latitude angle $\alpha = -30°$, longitude angle $\gamma = -30°$.

After all the targets in the queue list within the manipulator workspace at current platform position had been sprayed, a message of "duty accomplished" was generated by the sensing PC, and the platform was then moved by 200 mm to next step.

In order to assess the performance of the automatic disease-detection system, the algorithm output for each robotic pass was compared with the plant pathologist's visual inspection records (for position, size and intensity of symptoms). The final spray deposit on the canopy, and specifically on individual disease foci, was evaluated by spraying a

fluorescent water solution (Fluorescein sodium salt F6377, Sigma-Aldrich, Saint Louis, MO, USA) observed under ultraviolet light.

3.3. Description of the disease detection algorithm

The disease detection algorithm in R-G-NIR multispectral images was based on the spectral indices approach already introduced in Oberti et al. (2012) and detailed in Oberti et al. (2014). Spectral indices are algebraic combinations of pixel's grey levels in images acquired in two or more spectral channels, which can largely enhance the discrimination of disease symptoms from healthy tissue, being much less dependent than raw grey values in single channels on the level and homogeneity of illumination.

In particular, the combined use of the two spectral indices:

$$I1 = (R \cdot G) \Big/ \hat{NIR2} \quad (1)$$

$$I2 = R/(R + G + NIR) \quad (2)$$

was successfully tested on grapevine for powdery mildew detection under perfectly diffuse illumination conditions (Oberti et al., 2014).

In this study, the spectral indices detection was combined with a parallel approach based on local gradient in pixels' grey value. This additional approach was necessary to reinforce the classification robustness due to the partially limited illumination homogeneity of the imaged canopy area, despite the design effort spent on diffuse illumination apparatus. The general structure of the used algorithm is described in the following (see Fig. 6).

3.3.1. Foreground discrimination

The first step was the segmentation of the vegetation from the background in the acquired image. The presence of dark shield on the back of the prepared canopy resulted in a bimodal distribution of grey values in the NIR channel. This allowed an accurate segmentation of high grey levels for canopy foreground from low grey levels of the background by means of a Gaussian mixture fit on the histogram of grey levels in the NIR channel.

3.3.2. Spectral indices-based disease detection

For the segmented foreground, pair values of spectral indices I1 and I2, as defined in Eqs (1) and (2), were computed pixel by pixel. These two indices were designed to respond to major reflectance variations in tissue due to presence of fungal structures or to chlorophyll degradation in infected tissue and were expected to give significantly higher values for pixels in diseased areas compared to those obtained for healthy tissue pixels (Oberti et al., 2014).

The computed features pair were then used to classify the current pixel according to decision regions in the features plane (I1, I2). These are regions in which the plane was subdivided and that assign any possible combination of spectral indices (I1, I2) to one of the following classes: healthy tissue, powdery mildew infection, necrotic tissue, shoots/young branches, pigmented tissue other than disease (including glossy spot reflections).

The boundaries of decision regions used in this work have been defined by a training phase conducted on a calibration set of 12 images. These image were acquired on two reduced canopy setup prepared in a previous date (three weeks prior) and with different plant material than that subsequently used in the main experiment run on robotic selective spraying.

Within the calibration set, different sub-image areas containing only canopy regions corresponding to one of the considered classes were randomly selected. Inside each selected area, regions of interest (ROIs) at least 10 × 10 pixels wide were manually extracted, obtaining a total number of 50 ROIs healthy tissue, 30 ROIs of disease, 15 ROIs of necrotic tissue, 15 ROIs of shoots, and 10 ROIs of pigmentations other than disease, respectively.

The centroid of each class distribution in the features plane (I1, I2) was computed by averaging the corresponding representative data from the extracted ROIs. The plane was then divided in cells on the basis of a regular mesh grid, and for each grid cell the Euclidean distance measure from the class centroids was calculated. Each grid cell was finally assigned to the class at the closest distance, delimiting five decisions regions in the features plane.

The decision regions were implemented in the algorithm to select the foreground pixels with features (I1, I2) which corresponds to powdery mildew infection and to classify them as potentially diseased tissue.

3.3.3. Grey value gradient-based disease detection

The algorithm implements a concurrent approach based on gradient in pixels' grey value. This is applied to the I2 spectral index image, computed according to Eq. (2). In this image, the discrete disease infections were expected to appear as local regions with homogeneous grey (i.e. I2) values which significantly higher than the surrounding tissue.

To segment such regions, a seeded region growing method was applied starting from the local maxima found in the I2 image. Regions around the local maxima grow by including the surrounding pixels until the I2 value of a newly added pixel were within 10% of the region's average.

Once the growth stopped, then the contrast in mean grey value between the segmented region and the neighbour surrounding area was computed. Finally, the segmented regions found to have the computed contrast above a threshold (during the experiments a threshold contrast ratio of 1.4 was used) were classified as potentially diseased tissue.

3.3.4. Spraying targets detection

At the end of the two parallel classification processes, the detection algorithm combined the obtained disease maps by applying a logical AND combination of the outputs (i.e. it retained the regions for that the two methods agreed above a certain probability threshold) in order to obtain a disease binary mask. Finally a 3 × 3 binary opening filter was applied to remove noise pixels.

The binary regions left were then assumed to be detected disease areas and candidates to be sprayed by the robot, while the rest of the image foreground was assumed to correspond to vegetation that did not require spraying.

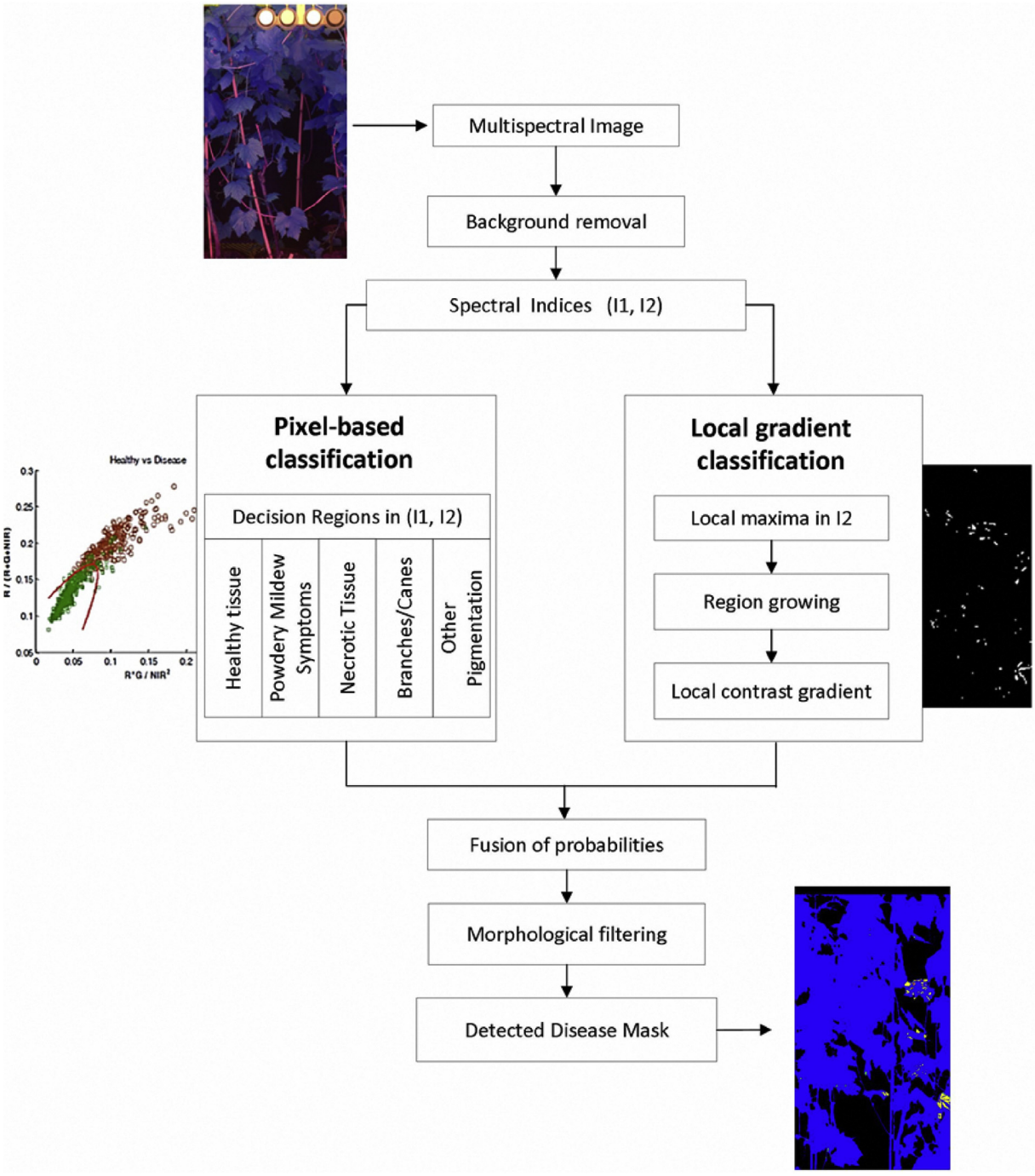

Fig. 6 – Disease detection algorithm block diagram.

3.4. *Spraying spots centring optimisation*

In order to minimise the number of spraying spots necessary to cover all the detected targets, the position of each spot, i.e. circles of 150 mm diameter, had to be optimised to enclose the largest number of sensed disease areas. To this aim, the target coordinate detected by the algorithm were grouped in pairs based on the condition of shortest Euclidean distance. When the two closest targets were grouped, a new macro-target was formed with coordinates centred at the mid-distance between the two original targets and radius given by the distance between them, increased by the original size of both.

The obtained macro-targets were now computed with other targets and grown further by aggregating additional targets using the process described above. A macro-target stopped growing when by adding the nearest target its radius exceeded 150 mm, i.e. its size would be larger than the area covered by a single spray spot.

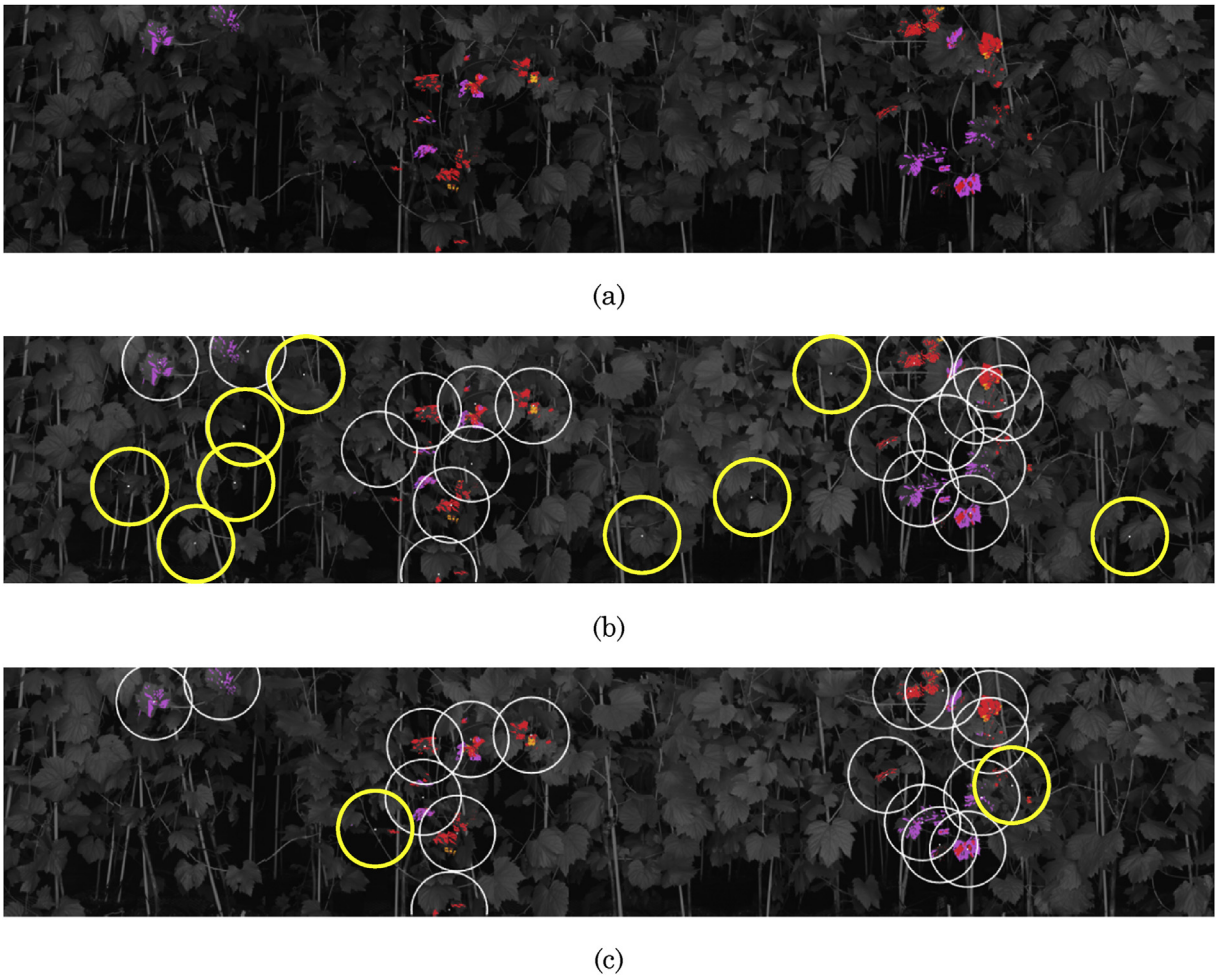

Fig. 7 – Summary of results obtained in experimental run 2. a) Disease area ground truth: in violet early symptoms of powdery mildew; in red middle symptoms; in orange advanced symptoms. b) spot sprayings operated by the robot during the pass; circles marked in yellow represent false positives, i.e. sprayings on healthy canopy erroneously classified as containing disease. c) spot sprayings minimally necessary to cover all the disease area computed from the ground truth; circles marked in yellow represent false negatives, i.e. disease that robot failed to detect and spray.

When all the detected targets were aggregated in macro-targets, the list of their centre coordinates was sent to the manipulator control for robotic spraying.

4. Results and discussion

The robotic system was tested on four different dates on four different grapevine canopy preparations which exhibited varying powdery mildew disease symptom levels and spreading densities within the foliage. The operative results obtained with robotic selective spraying of disease symptoms were quantitatively assessed through: a) the *sensitivity* of the selective treatment, i.e. the capability of covering real targets (fraction of disease area which was sprayed by the robot); b) the *specificity* of the selective treatment which expressed the capability of avoiding excess spraying (i.e. canopy area not requiring spraying which was left unsprayed by the robot); c) the potential *pesticide reduction* obtained by selective spraying was expressed as the reduction of pesticide used compared to a conventional uniform spray distribution operated at the same application rate.

As an illustrative example, in Fig. 7 the results obtained for one of the prepared canopy plots (experimental run 2) are shown. The figure refers to a vegetation area about 4.2 m wide and 0.75 m high and it displays the canopy as it was sensed by the robot during its passage; indeed, the canopy map shown was obtained by aligning the multispectral camera images (in particular, R + G + NIR grey levels) acquired at steps of 200 mm by the robot.

In Fig. 7a the position and size of disease foci as obtained by a plant pathologist's survey (ground truth) are displayed on grapevine canopy as coloured areas. Each colour corresponds to a different stage of the disease symptoms as they were diagnosed by the human expert: violet areas are early symptoms of infection; in red are middle symptoms; in orange are advanced symptoms; uncoloured area corresponds to healthy vegetation.

Regardless to the infection stage, the area covered by disease in this plot was 8.9% of the total canopy area. For the goal

of the experiment, these coloured regions represent the real targets of selective spraying.

Figure 7b shows circles corresponding to where spot sprayings were operated by the robot during the pass, as final result of the detection process and manipulator control actuation. The robot sprayed 27 spots that covered 95% of the disease area. It is noticeable that all the diseased portions of the canopy (i.e., the two main disease foci in middle and at right side of the image, and the small infected area on left upper side) were detected and treated by robot.

As a benchmark, Fig. 7c shows the spot sprayings minimally necessary to cover all the disease area, as they were computed from the pathologist survey (i.e., from ground truth in Fig. 7a). By comparing Fig. 7b and c, it can be seen that in this specific run the robot failed to detect and treat two small disease symptoms (corresponding to the uncovered 5% of the disease area) represented by the two marked circles in Fig. 7c. On the other hand, 9 of the 27 spots sprayed by the robot (marked circles in Fig. 7b) were targeted on false positives, i.e. on healthy canopy erroneously classified as containing some disease. A detailed analysis of false positives revealed that specular reflection spots due to the illumination system were a major cause factor. This indicates that obtaining a highly diffused illumination of the imaged area was a crucial issue to be addressed for limiting false positive rates in the adopted disease detection system.

As a result, robotic selective spraying gave a pesticide reduction of 64% when compared to a conventional homogeneous spraying of the canopy, assuming to adopt the same application rate; i.e., only the 36% of the pesticide used in corresponding conventional treatment was used by the robot. As reference for this case, a potential pesticide reduction of 75% could have been attained by actuating the optimal spraying spots computed on the basis of the ground-truth data.

Table 2 summaries the results of robotic selective spraying on the four different grapevine canopy preparations.

With run 1, a scenario characterised by a small yet sparse disease area (1.6% of the foliage) was investigated. During this run the robot reached its maximum sensitivity with the 100% of the targets covered by spraying. The specificity of the system was nevertheless limited, since 15 of the 25 sprayed spots were false positives. The obtained pesticide reduction vs. homogeneous treatment was 84%, to be compared with a potential reduction of 94% by optimal spraying spots computed on the ground-truth data.

Run 3 (disease area 9.1%) was conducted on an experimental situation similar to the above discussed run 2 obtaining comparable results.

In run 4 different grapevine plants presenting pigmentation due to nutritional disorders (not powdery mildew disease) were intentionally included in the canopy preparation to represent an area potentially corresponding to a high-density source of false positives. Noticeably, the overall results of run 4 were not significantly different from those obtained in other runs, showing that the detection system resulted robust enough for rejecting this kind of false positives.

False negatives (undetected/unsprayed disease symptoms) were mostly located in the surrounding of detected disease areas. This indicates that they could be treated anyway if a conservative buffer area around the spot spraying targets would be included. Despite this will reduce the potential pesticide savings, it might help to raise the level of acceptance in to real-world application of selective spraying systems.

An even more advanced approach at this level could integrate a disease-specific epidemic model aimed at estimating the probable area of latent infections around the detected symptoms, and to consequently better adjust the spraying radius. Nevertheless, this possible improvement is beyond the goal of this particular work and is left for future research.

5. Conclusions

This study investigated the feasibility of automatically detecting the symptoms of powdery mildew, a major fungal grapevine disease, and of selectively spraying the diseased canopy areas.

To this aim, the CROPS modular agricultural robot was equipped with a precision-spraying end-effector and configured for this application. A disease-sensing system based on multispectral imaging and associated detection algorithm was integrated with real-time manipulator control in a ROS based communication framework.

The robotic system was tested on four different grapevine canopy preparations, which exhibited varying powdery

Table 2 – Summary of results of robotic selective spraying on four different grapevine canopy plots exhibiting varying powdery mildew disease symptom levels and spread density. For experiment 4 plants with nutritional disorders as possible false positives were intentionally added.

Experiment run	Diseased area	Number of spray spots		Disease sprayed		Pesticide reduction	
		Robot	*Optimal*	Robot	*Optimal*	Robot	*Optimal*
Run 1	1.6%	25	10	100%	100%	84%	94%
Run 2	8.9%	27	19	95%	100%	64%	75%
Run 3	9.1%	31	23	85%	100%	63%	73%
Run 4[a]	4.2%	21	14	86%	100%	75%	83%

[a] High density of false positives sources intentionally added.

mildew disease symptom levels and spread density within the foliage. The results obtained in the experiments carried indicate that the CROPS robot was able:

- to treat from 85% to 100% of the disease area within the canopy;
- to limit the healthy area unintentionally sprayed (false positive) from 5% to 20% of the total canopy area;
- to reduce the pesticide of about 65%–85% (depending on disease levels and spatial distribution of foci) when compared to a conventional homogeneous spraying of the canopy.

Moreover

- for all the cases, the obtained pesticide reduction was close to the 90% of the maximum potential reduction (computed as the spot sprayings strictly necessary to treat all the real disease symptoms);
- the major source of false positives appears to be associated to specular reflections spots on glossy leaf tissue, indicating that obtaining a highly diffused illumination of the imaged area is a crucial issue for adopted disease detection system.

To the best of our knowledge, this is the first experiment conducted on totally automatic, selective spraying of diseases in specialty crops.

Acknowledgements

The CROPS project (GA-246252) was funded by the European Commission under the 7th Framework Programme within the theme "Automation and robotics for sustainable crop and forestry management".

REFERENCES

Abdollahi, M., Ranjbar, A., Shadnia, S., Nikfar, S., & Rezaie, A. (2004). Pesticides and oxidative stress: a review. *Medical Science Monitor, 10*, RA141–RA147.

Bac, C. W., van Henten, E. J., Hemming, J., & Edan, Y. (2014). Harvesting robots for high-value crops: state-of-the-art review and challenges ahead. *Journal of Field Robotics, 31*, 888–911.

Baeten, J., Donné, K., Boedrij, S., Beckers, W., & Claesen, E. (2008). Autonomous fruit picking machine: a robotic apple harvester. *Tracts in Advanced Robotics, 42*, 531–539.

Baur, J., Pfaff, J., Ulbrich, H., & Villgrattner, T. (2012). Design and development of a redundant modular multipurpose agricultural manipulator. *IEEE/ASME Advanced Intelligent Mechatronics (AIM), 2012*, 823–830. http://dx.doi.org/10.1109/AIM.2012.6265928.

Bélanger, M. C., Roger, J. M., Cartolaro, P., Viau, A. A., & Bellon-Maurel, V. (2008). Detection of powdery mildew in grapevine using remotely sensed UV-induced fluorescence. *International Journal of Remote Sensing, 29*, 1707–1724.

Belforte, G., Deboli, R., Gay, P., Piccarolo, P., & Ricauda Aimonino, D. (2006). Robot design and testing for greenhouse applications. *Biosystems Engineering, 95*, 309–321.

Bontsema, J., Hemming, J., Pekkeriet, E., Saeys, W., Edan, Y., Shapiro, A., et al. (2014). CROPS: high tech agricultural robots. In *Proc. Int. Conf. Agricultural Engineering, AgEng2014-Zurich (CH), paper C0141*. ISBN: 978-0-9930236-0-6.

Burns, C. J., McIntosh, L. J., Mink, P. J., Jurek, A. M., & Li, A. A. (2013). Pesticide exposure and neurodevelopmental outcomes: review of the epidemiologic and animal studies. *Journal of Toxicology and Environmental Health – Part B: Critical Reviews, 16*, 127–183.

Calcante, A., Mena, A., & Mazzetto, F. (2012). Evaluation of "ground sensing" optical sensors for diagnosis of Plasmopara viticola on vines. *Spanish Journal of Agricultural Research, 10*, 619–630.

Everhart, S. E., Askew, A., Seymour, L., & Scherm, H. (2013). Spatio-temporal patterns of pre-harvest brown rot epidemics within individual peach tree canopies. *European Journal of Plant Pathology, 135*, 499–508.

Felton, W. L., & McCloy, K. R. (1992). Spot spraying. *Agricultural Engineering, 73*, 9–12.

Guo, J., Zhao, D., Ji, W., & Xia, W. (2010). Design and control of the open apple-picking-robot manipulator. In *Proc. IEEE Int. Conf. on Computer Science and Information Technology (ICCSIT)* (vol. 2, pp. 5–8).

Hayashi, S., Shigematsu, K., Yamamoto, S., Kobayashi, K., Kohno, Y., Kamata, J., et al. (2010). Evaluation of a strawberry-harvesting robot in a field test. *Biosystems Engineering, 105*, 160–171.

Hayashi, S., Yoshida, H., Yamamoto, S., Iwasaki, Y., & Urushiyama Miyagi, Y. (2008). Design of a strawberry factory using a movable bench. *Acta Horticulturae, 801*, 653–659.

Katupitiya, J., Eaton, R., Cole, A., Meyer, C., & Rodnay, G. (2005). Automation of an agricultural tractor for fruit picking. In *Proc. IEEE Int. Conf. on Robotics and Automation (ICRA)* (pp. 3201–3206).

Larbi, P. A., Ehsani, R., Salyani, M., Maja, J. M., Mishra, A., & Camargo Neto, J. (2013). Multispectral-based leaf detection system for spot sprayer application to control citrus psyllids. *Biosystems Engineering, 116*, 509–517.

Lee, W. S., Alchanatis, V., Yang, C., Hirafuji, M., Moshou, D., & Li, C. (2010). Sensing technologies for precision specialty crop production. *Computers and Electronics in Agriculture, 74*, 2–33.

Li, G. L., Ma, Z. H., & Wang, H. G. (2012). Image recognition of grape downy mildew and grape powdery mildew based on support vector machine. In V. D. Li, & Y. Chen (Eds.), *Computer and computing technologies in agriculture* (vol. 370, pp. 151–162). Springer Berlin Heidelberg.

Li, Y., Xia, C., & Lee, J. (2009). Vision-based pest detection and automatic spray of greenhouse plant. In *IEEE International Symposium on Industrial Electronics, Proc. ISIE 2009* (pp. 920–925). http://dx.doi.org/10.1109/ISIE.2009.5218251.

Mahlein, A. K., Oerke, E. C., Steiner, U., & Dehne, H. W. (2012). Recent advances in sensing plant diseases for precision crop protection. *European Journal of Plant Pathology, 133*, 197–209.

Malneršič, A., Hočevar, M., Širok, B., Marchi, M., Tirelli, P., & Oberti, R. (2012). Close range precision spraying airflow/plant interaction. In *Proc. of the First RHEA International Conference on Robotics and associated High-technologies and Equipment for Agriculture, Pisa 2012*. ISBN: 9788867410217.

Mandow, A., Gomez-de-Gabriel, J., Martinez, J., Munoz, V., Ollero, A., & Garcia-Cerezo, A. (1996). The autonomous mobile robot AURORA for greenhouse operation. *Robotics Automation Magazine, IEEE, 3*, 18–28.

Moshou, D., Bravo, C., Oberti, R., West, J. S., Ramon, H., Vougioukas, S., et al. (2011). Intelligent multi-sensor system for the detection and treatment of fungal diseases in arable crops. *Biosystems Engineering, 108*, 311–321.

Naidu, R. A., Perry, E. M., Pierce, F. J., & Mekuria, T. (2009). The potential of spectral reflectance technique for the detection of Grapevine leafroll-associated virus-3 in two red-berried wine

grape cultivars. *Computers and Electronics in Agriculture, 66*, 38–45.
Oberti, R., Marchi, M., Tirelli, P., Calcante, A., Iriti, M., & Borghese, A. N. (2014). Automatic detection of powdery mildew on grapevine leaves by image analysis: optimal view-angle range to increase the sensitivity. *Computers and Electronics in Agriculture, 104*, 1–8.
Oberti, R., Tirelli, P., Marchi, M., Calcante, A., Iriti, M., & Borghese, N. A. (2012). Automatic diseases detection in grapevine under field conditions. In *Proc. of the First RHEA International Conference on Robotics and associated High-technologies and Equipment for Agriculture, Pisa 2012*. ISBN: 9788867410217.
Paice, M. E. R., Miller, P. C. H., & Day, W. (1996). Control requirements for spatially selective herbicide sprayers. *Computers and Electronics in Agriculture, 14*, 163–177.
Pfaff, J., Baur, J., Ulbrich, H., & Villgrattner, T. (2012). Development of a multipurpose agricultural manipulator. In *Proc. of the First RHEA International Conference on Robotics and associated High-technologies and Equipment for Agriculture, Pisa 2012*. ISBN: 9788867410217.
Poutaraud, A., Latouche, G., Martins, S., Meyer, S., Merdinoglu, D., & Cerovic, Z. G. (2007). Fast and local assessment of stilbene content in grapevine leaf by in vivo fluorometry. *Journal of Agricultural and Food Chemistry, 55*, 4913–4920.
Quigley, M., Conley, K., Gerkey, B. P., Faust, J., Foote, T., Leibs, J., et al. (2009). *Ros: An open-source robot operating system*. ICRA Workshop on Open Source Software.
Rauh, V. A., Perera, F. P., Horton, M. K., Whyatt, R. M., Bansal, R., Hao, X., et al. (2012). Brain anomalies in children exposed prenatally to a common organophosphate pesticide. *PNAS, 109*, 7871–7876.
Sabatier, P., Poulenard, J., Fangeta, B., Reyss, J.-L., Develle, A.-L., Wilhelm, B., et al. (2014). Long-term relationships among pesticide applications, mobility, and soil erosion in a vineyard watershed. *PNAS, 111*, 15647–15652.
Sankaran, S., Mishra, A., Ehsani, R., & Davis, C. (2010). A review of advanced techniques for detecting plant diseases. *Computers and Electronics in Agriculture, 72*, 1–13.
Schütz, C., Pfaff, J., Baur, J., Buschmann, T., & Ulbrich, H. (2014). A modular robot system for agricultural applications. In *Proc. Int. Conf. Agricultural Engineering, AgEng2014-Zurich (CH), paper C0310*. ISBN: 978-0-9930236-0-6.
Siciliano, B., Sciavicco, L., & Villani, L. (2009). *Robotics: Modelling, planning and control*. Springer Verlag.
Slaughter, D. C., Giles, D. K., & Tauzer, C. (1999). Precision offset spray system for roadside weed control. *Journal of Transportation Engineering, ASCE, 125*, 364–371.
Spósito, M. B., Amorim, L., Bassanezi, R. B., Filho, A. B., & Hau, B. (2008). Spatial pattern of black spot incidence within citrus trees related to disease severity and pathogen dispersal. *Plant Pathology, 57*, 103–108.
Stehle, S., & Schulz, R. (2015). Agricultural insecticides threaten surface waters at the global scale. *PNAS, 112*, 5750–5755.
Van Henten, E. J., Van Tuijl, B. A. J., Hemming, J., Kornet, J. G., Bontsema, J., & Van Os, E. A. (2003). Field test of an autonomous cucumber picking robot. *Biosystems Engineering, 86*, 305–313.
Waggoner, P. E., & Aylor, D. E. (2000). Epidemiology: a science of patterns. *Annual Review of Phytopathology, 38*, 71–94.
West, J. S., Bravo, C., Oberti, R., Lemaire, D., Moshou, D., & McCartney, H. A. (2003). The potential of optical canopy measurement for targeted control of field crop diseases. *Annual Review of Phytopathology, 41*, 593–614.